An enhanced error estimator on the constitutive relation for plasticity problems

L. Gallimard, P. Ladevèze, J.P. Pelle

An enhanced error estimator on the constitutive relation for plasticity problems

L. Gallimard *, P. Ladevèze, J.P. Pelle

LMT – Cachan, ENS Cachan/CNRS/Univ. Paris 6, 61 avenue du Président Wilson, 94235 Cachan Cedex, France

Received 19 March 1999; accepted 18 February 2000

Abstract

This paper presents an extension to plasticity problems of a new error estimator on the constitutive relation which was introduced by P. Ladevèze in a recent paper. Numerical experiments show that this enhanced error estimator can lead to a significant improvement in the effectivity indexes in the case of anisotropic meshes, or when perfect plasticity is approached.

Keywords: Finite element method; Error estimator; Plasticity; Statically admissible stress fields; Error on the constitutive relation; Effectivity indexes

1. Introduction

One important research topic is the mastering of Finite Element (FE) analysis in plasticity calculations [1,2,5,6,10,12,13,17–21]. For such calculations, the quality of the finite element solution at t depends not only on the quality of the mesh, but also on the quality of the time discretization used since the beginning of the loading. Mastering such an analysis is thus clearly more complex than in the case of linear static problems. In particular, an approach which consists of directly applying at certain time steps the procedures used in statics is insufficient to estimate the quality of such a calculation. Therefore, to master a plasticity calculation, it is necessary to define error measures that allow to take into account all discretization errors over the whole time interval $[0, T]$. Error measures possessing these properties have been developed from an a posteriori error estimator based on the error on the constitutive relation [10]. Here, we will consider what we call Drucker's error estimator [10,4,5]. Other estimators were developed subsequently in Refs. [12,13]. Drucker's error estimator uses the same technique as in linear analysis for constructing the equilibrated stress fields; this technique is independent of the constitutive relation. However, the quality of our error estimator depends on the quality of the equilibrated stress field recovery. In order to improve the quality of our estimate, we present an enhanced construction technique derived from Ref. [15] which minimizes the constitutive relation error over the time-space domain and takes into account the constitutive relation. This new and enhanced construction leads to an enhanced Drucker's error estimator which is introduced here. The outline of this paper is as follows: In Section 2, the notations for a nonlinear evolution problem are introduced and in Section 3 the reader is reminded of the definition of the error on the constitutive relation. Section 4 outlines the standard construction of the equilibrated stress fields, and introduces the new construction which leads to an enhanced Drucker's error estimator for plasticity problems. In Section 5, the definition of our standard Drucker's error estimator is recalled, then we introduce the definition of an enhanced Drucker's error estimator. In Section 6, we detail the construction of the statistically admissible (SA) stress field. Finally, numerical simulations are performed with six-node triangular elements and the results are given in Section 7.

* Corresponding author. Fax: +33-1-4740-2785.
E-mail address: gallimar@lmt.ens-cachan.fr (L. Gallimard).

2. Reference problem to be solved

Let us assume that the structure is a domain Ω bounded by $\partial\Omega$, which is independent of t. Over the time interval $[0, T]$, the structure is submitted to

- a prescribed displacement $\underline{U}_d(\underline{M}, t)$ on a portion $\partial_1\Omega$ of the boundary,
- a traction $\underline{F}_d(\underline{M}, t)$ on the complementary portion $\partial_2\Omega$,
- a distribution of body forces $\underline{f}_d(\underline{M}, t)$ on the domain Ω.

In a time-dependent nonlinear calculation, the value of the stress at time t is a function of the history of the strain until time t, which can be defined, at each point M of the structure Ω, by the relation:

$$\boldsymbol{\sigma}(\underline{M}, t) = \mathbf{A}(\boldsymbol{\varepsilon}(\dot{\underline{U}}\ (\underline{M}, \tau));\ \tau \leqslant t), \tag{1}$$

where $\mathbf{A}$ is an operator characteristic of the material and $\boldsymbol{\varepsilon}$ is the strain field.

Let us designate by $\mathscr{U}_{\text{ad}}^{[0,T]}$, the space of the displacements satisfying the kinematic constraints:

$$\begin{aligned}\mathscr{U}_{\text{ad}}^{[0,T]} = \{&\underline{U}(\underline{M}, t) \in \mathscr{U}^{[0,T]} \text{ such that } \underline{U}\,|_{\partial_1\Omega}\ (\underline{M}, t) \\ &= \underline{U}_d(\underline{M}, t)\ \forall\ t \in [0, T]\},\end{aligned} \tag{2}$$

where $\mathscr{U}^{[0,T]}$ is the space of the displacement fields $\underline{U}(\underline{M}, t)$ defined on $\Omega \times [0, T]$ and let us designate by $\mathscr{S}_{\text{ad}}^{[0,T]}$, the space of stresses which are solutions to the equilibrium equations:

$$\begin{aligned}\mathscr{S}_{\text{ad}}^{[0,T]} = \Bigg\{&\boldsymbol{\sigma}(\underline{M}, t) \in \mathscr{S}^{[0,T]} \text{ such that } \quad \forall\ \underline{U}^* \in \mathscr{U}_0\ \forall\ t \in [0, T] \\ &\int_\Omega \text{tr}[\boldsymbol{\sigma}\boldsymbol{\varepsilon}(\underline{U}^*)]\,\mathrm{d}\Omega = \int_\Omega \underline{f}_d^T \underline{U}^*\,\mathrm{d}\Omega + \int_{\partial_2\Omega} \underline{F}_{\text{d}}^T \underline{U}^*\,\mathrm{d}S\Bigg\},\end{aligned} \tag{3}$$

where $\mathscr{U}_0 = \{\underline{\mathbf{U}}(\mathbf{M}, \mathbf{t}) \in \mathscr{U}^{[0,T]} \text{ such that } \underline{\mathbf{U}}\,|_{\partial_1\Omega} = 0\}$ and $\mathscr{S}^{[0,T]}$ is the space of the stress fields $\boldsymbol{\sigma}(\underline{M}, t)$.

The nonlinear problem can then be formulated in the following manner:

$$\begin{aligned}\text{Find } (U(\underline{M}, t), \boldsymbol{\sigma}(\underline{M}, t)) \in\ &\mathscr{U}_{\text{ad}}^{[0,T]} \\ &\times \mathscr{S}_{\text{ad}}^{[0,T]} \text{ that satisfies Eq. (1).}\end{aligned} \tag{4}$$

3. Error on the constitutive relation – principle

For models which satisfy Drucker's inequality [3] strictly, the error on the constitutive relation was introduced in Ref. [8] and associated error estimators appeared in Refs. [4,5,10]. The principle of the error on the constitutive relation [7,10,11] relies on separating the equations of the problem into two groups. In what we call Drucker's error estimator, the first group of equations combines the kinematic constraints (2) with the equilibrium equation (3) (i.e. $\mathscr{U}_{\text{ad}}^{[0,T]} \times \mathscr{S}_{\text{ad}}^{[0,T]}$), and the second group contains the constitutive relation (1).

3.1. Druckers's inequality

Let $(\boldsymbol{\varepsilon}, \boldsymbol{\sigma})$ and $(\boldsymbol{\varepsilon}', \boldsymbol{\sigma}')$ be two arbitrary strain–stress pairs which satisfy the constitutive relation described in Eq. (1) on $[0, T]$, with $(\boldsymbol{\varepsilon}, \boldsymbol{\sigma}) = (\boldsymbol{\varepsilon}', \boldsymbol{\sigma}') = (0, 0)$ at $t = 0$. The material is said to satisfy Drucker's inequality if it satisfies Eq. (5). Moreover, if Eq. (6) is satisfied, the material is said to satisfy Drucker's stability inequality strictly.

$$\forall\, t \in [0, T] \int_0^t \text{tr}[(\boldsymbol{\sigma} - \boldsymbol{\sigma}')(\dot{\boldsymbol{\varepsilon}} - \dot{\boldsymbol{\varepsilon}}')]\,\mathrm{d}t \geqslant 0, \tag{5}$$

$$\begin{aligned}&\forall\, t \in [0, T] \int_0^t \text{tr}[(\boldsymbol{\sigma} - \boldsymbol{\sigma}')(\dot{\boldsymbol{\varepsilon}} - \dot{\boldsymbol{\varepsilon}}')]\,\mathrm{d}t = 0 \\ &\quad\Longleftrightarrow\ \forall\, t \in [0, T](\boldsymbol{\varepsilon}, \boldsymbol{\sigma}) = (\boldsymbol{\varepsilon}', \boldsymbol{\sigma}').\end{aligned} \tag{6}$$

Note that in Ref. [9], it is shown that Eqs. (5) and (6) are verified for most practical plasticity and viscoplasticity models. Moreover, in Ref. [9], it has been proved that for such models the solution to the reference problem to be solved is unique.

3.2. The Drucker error on the constitutive relation

Let $s_{\text{ad}} = (\underline{U}_{\text{KA}}, \boldsymbol{\sigma}_{\text{SA}})$ be an admissible pair belonging to $\mathscr{U}_{\text{ad}}^{[0,T]} \times \mathscr{S}_{\text{ad}}^{[0,T]}$, and let us define the scalar quantity.

$$\begin{aligned}\eta(\underline{M}, t, s_{\text{ad}}) \equiv \int_0^t\ &\text{tr}[(\boldsymbol{\sigma}_{\text{SA}}(\underline{M}, t) - \boldsymbol{\sigma}_{\text{KA}}(\underline{M}, t)) \\ &\times (\dot{\boldsymbol{\varepsilon}}_{\text{SA}}(\underline{M}, t) - \boldsymbol{\varepsilon}(\dot{\underline{U}}_{\text{KA}}(\underline{M}, t))]\,\mathrm{d}t,\end{aligned} \tag{7}$$

where $\boldsymbol{\sigma}_{\text{KA}}$ is the stress field related to the displacement $\underline{U}_{\text{KA}}$ through the constitutive relation (1) on $\Omega \times [0, T]$, and $\boldsymbol{\varepsilon}_{\text{SA}}$ is the strain field related to $\boldsymbol{\sigma}_{\text{SA}}$.

For a material which satisfies Drucker's inequality strictly,

- $\eta(\underline{M}, t, s_{\text{ad}})$ is positive or zero on $\Omega \times [0, T]$,
- $\eta(\underline{M}, t, s_{\text{ad}}) = 0$ on $\Omega \times [0, T]$ if and only if $(\underline{U}_{\text{KA}}, \boldsymbol{\sigma}_{\text{SA}})$ is the exact solution to the reference problem (4).

To evaluate the quality of $(\underline{U}_{\text{KA}}, \boldsymbol{\sigma}_{\text{SA}})$ as an approximate solution to the model problem, the previous relations lead us to define the following *time-global* error measure at T:

$$e_T = \sup_{t \in [0,T]} e[0, t], \tag{8}$$

where the contribution to the error over $[0, t]$ is

$$e^2[0, t]\ = \int_\Omega \eta(\underline{M}, t, s_{\text{ad}})\,\mathrm{d}\Omega. \tag{9}$$

The relative error is given by

$$\varepsilon_T = \sup_{t\in[0,T]} e[0,t]/D,$$

$$D^2 = 2\int_0^{\mathrm{T}} \int_\Omega \left[\mathrm{tr}[\boldsymbol{\sigma}_{\mathrm{KA}}\dot{\boldsymbol{\varepsilon}}_{\mathrm{KA}}] + \mathrm{tr}[\boldsymbol{\sigma}_{\mathrm{SA}}\ \dot{\boldsymbol{\varepsilon}}_{\mathrm{SA}}]\right] \mathrm{d}\Omega\,\mathrm{d}t. \qquad (10)$$

This includes all sources of error: space discretization, time discretization, ...

The next section discusses the technique for constructing an admissible pair $(\underline{U}_{\mathrm{KA}}, \boldsymbol{\sigma}_{\mathrm{SA}})$ from a finite element solution and from the data.

4. Recovery of SA stress and kinematically admissible (KA) displacement on $\Omega \times [0, T]$

4.1. Finite element solution

Within the framework of the FEM, an approximate solution to problem (4) is obtained by using an incremental method along with a finite element discretization $\mathbf{E}$ and a time discretization Δ.

Assuming that the histories of both displacements and stresses are known until t_{i-1}, then the problem is to compute these histories on the increment $[t_{i-1}, t_i]$ (with $\Delta = \{t_1, \ldots, t_n\}$ and $t_1 = 0 < t_2 < \cdots < t_{n-1} < t_n = T$). A number of algorithms using a displacement approach are available to solve this problem [16].

At the end of each time increment t_i, these algorithms provide

- a finite element displacement field which satisfies the kinematic constraints,

$$\underline{U}_h(\underline{M}, t_i) = N(\underline{M})^{\mathrm{T}}\, \underline{q}(t_i), \qquad (11)$$

  where $N(\underline{M})$ designates the matrix of the shape functions and $\underline{q}(t_i)$ the vector of the nodal displacements at t_i,
- a stress field $\boldsymbol{\sigma}_h(\underline{M}, t_i)$ which satisfies the equilibrium equations of the finite element model at t_i,
- a stress field $\tilde{\boldsymbol{\sigma}}_h(\underline{M}, t_i)$ which is linked to $\underline{U}_h(\underline{M}, t_i)$ by the constitutive relation.

Assuming that the data are piecewise linear on $[0, T]$, it is easy to complete the FE solution on $[0, T]$ in order to obtain both a displacement $\underline{U}_h(\underline{M}, t)$ that satisfies the kinematic constraints and a stress field $\boldsymbol{\sigma}_h(\underline{M}, t)$ that satisfies the equilibrium equations of the finite element model on $[0, T]$.

4.2. Recovery of KA displacement on $\Omega \times [0, T]$

Since the displacement $\underline{U}_h(\underline{M}, t)$ satisfies the kinematic constraints (2), the displacement $\underline{U}_{\mathrm{KA}}(\underline{M}, t)$ can be obtained easily,

$$\underline{U}_{\mathrm{KA}}(\underline{M}, t) = \underline{U}_h(\underline{M}, t). \qquad (12)$$

4.3. Standard recovery of SA stresses on $\Omega \times [0, T]$

The objective is to calculate the stress $\boldsymbol{\sigma}_{\mathrm{SA}}(\underline{M}, t)$ belonging to $\mathscr{S}_{\mathrm{ad}}^{[0,T]}$. In Ref. [4], we applied the method introduced by Ladevèze in Ref. [7]. This method is based on a prolongation condition used to link $\boldsymbol{\sigma}_{\mathrm{SA}}(\underline{M}, t_i)$ to the finite element stress $\boldsymbol{\sigma}_h(\underline{M}, t_i)$:

$$\forall E \in \mathbf{E}\ \forall j \in \mathbf{I} \int_E \mathrm{tr}[(\boldsymbol{\sigma}_{\mathrm{SA}}(\underline{M}, t_i) - \boldsymbol{\sigma}_h(\underline{M}, t_i))\, \boldsymbol{\varepsilon}(\underline{\omega}_j)]\, \mathrm{d}\Omega = 0, \qquad (13)$$

where $\mathbf{E}$ is set of mesh elements, $\mathbf{I}$ is the set of nodes and $\underline{\omega}_j$ are the shape functions.

The stress $\boldsymbol{\sigma}_{\mathrm{SA}}(\underline{M}, t)$ is evaluated in two steps:

- In the first step, we determine on the edge of each element E the element tractions $\widehat{\underline{F}}_h(t_i)$ which equilibrate the data. These distributions are obtained as a linear combination of the shape functions.
- In the second step, the statically admissible stress field is built on each element E from the element tractions $\widehat{\underline{F}}_h(t_i)$. Then it is easy to complete $\boldsymbol{\sigma}_{\mathrm{SA}}(\underline{M}, t_i)$ in order to obtain a solution $\boldsymbol{\sigma}_{\mathrm{SA}}(\underline{M}, t) \in \mathscr{S}_{\mathrm{ad}}^{[0,T]}$ (under the assumption that the data are piecewise linear over $[0, T]$).

This method used in Ref. [4] involves only local calculations and is independent of the constitutive relation. However, it is clear that the quality of our error measure is closely related to the quality of the force distribution $\widehat{\underline{F}}_h(t_i)$. The projections of $\widehat{\underline{F}}_h(t_i)$ on the shape functions associated with nonvertex nodes are determined uniquely by Eq. (13). In contrast, some indeterminate quantities appear in the projections associated with the vertex nodes. These indeterminate quantities are resolved by the introduction of a cost function which does not necessarily lead to the best error estimator. Further details on this construction are provided in Ref. [14].

4.4. Enhanced recovery of SA stresses on $\Omega \times [0, T]$: principle

An improvement in the recovery method of SA stresses has been developed in Ref. [15]. Here, we show how to extend this new method to plasticity problems.

We will assume, as in Section 4.3, that the data are piecewise linear over $[0, T]$ (an assumption which in practice is not restrictive). Therefore, we will focus on the construction of $\boldsymbol{\sigma}_{\mathrm{SA}}^{\mathrm{ENH}}(\underline{M}, t_i)$ (for $t_i \in [0, T]$), where $\boldsymbol{\sigma}_{\mathrm{SA}}^{\mathrm{ENH}}(\underline{M}, t)$ is obtained by linear interpolation.

Following Ref. [15], we introduce a weak prolongation condition in order to link the SA stress to the FE stress.

$$\forall E \in \mathbf{E}\ \forall j \in \bar{\mathbf{I}} \subset \mathbf{I} \int_E \mathrm{tr}[(\boldsymbol{\sigma}_{\mathrm{SA}}^{\mathrm{ENH}}(\underline{M}, t_i) - \boldsymbol{\sigma}_h(\underline{M}, t_i))\, \boldsymbol{\varepsilon}(\underline{\omega}_j)]\, \mathrm{d}\Omega = 0, \qquad (14)$$

where $\bar{\mathbf{I}}$ is associated with the nonvertex nodes.

Let us designate by $\mathscr{S}_{\text{ad}}^{t_i}$ the space of the stresses which satisfy the equilibrium equations at t_i:

$$\mathscr{S}_{\text{ad}}^{t_i} = \Big\{ \boldsymbol{\sigma} \in \mathscr{S} \text{ such that } \quad \forall\, \underline{U}^* \in \mathscr{U}_0 \int_\Omega \text{tr}[\boldsymbol{\sigma}\, \boldsymbol{\varepsilon}(\underline{U}^*)]\, \mathrm{d}\Omega = \int_\Omega \underline{f}_d(\underline{M}, t_i)^{\mathrm{T}} \underline{U}^*\, \mathrm{d}\Omega + \int_{\partial_2\Omega} \underline{F}_d(\underline{M}, t_i)^{\mathrm{T}} \underline{U}^*\, \mathrm{d}S \Big\}, \tag{15}$$

where $\mathscr{S}$ is the space of the stress fields.

Define by $\mathscr{S}_{\text{ad},h}^{\Delta}$ the set of stresses:

$$\mathscr{S}_{\text{ad},h}^{\Delta} = \{ \{ \boldsymbol{\sigma}(\underline{M}, t_1), \ldots, \boldsymbol{\sigma}(\underline{M}, t_n) \} \in \mathscr{S}^n \text{ such that } \forall i \in \{1, \ldots, n\} \quad \boldsymbol{\sigma}(\underline{M}, t_i) \in \mathscr{S}_{\text{ad}}^{t_i} \text{ and } \boldsymbol{\sigma}(\underline{M}, t_i) \text{ satisfies Eq. (14)} \}. \tag{16}$$

$\boldsymbol{\sigma}_{\text{SA}}^{\text{ENH}}(\underline{M}, t_i)$ $(\forall i \in \{1, \ldots, n\})$ is obtained by solving the following minimization problem:

$$\text{Find} \{ \boldsymbol{\sigma}_{\text{SA}}^{\text{ENH}}(\underline{M}, t_1), \ldots, \boldsymbol{\sigma}_{\text{SA}}^{\text{ENH}}(\underline{M}, t_n) \} \in \mathscr{S}_{\text{ad},h}^{\Delta} \text{that minimizes the error on the constitutive relation } e_T \text{ defined in Eq. (8).} \tag{17}$$

This explains why this new version is better than the previous one; the recovered equilibrated stress is better.

5. Standard and enhanced Drucker's error estimators

5.1. Standard Drucker's error estimator

The standard Drucker's error estimator is defined as in [4]:

$$e_T = \sup_{t \in [0,T]} \left(\int_\Omega \eta(\underline{M}, t, s_{\text{ad}}^{\text{STD}})\, \mathrm{d}\Omega \right), \tag{18}$$

where $s_{\text{ad}}^{\text{STD}} = (\underline{U}_{\text{KA}}, \boldsymbol{\sigma}_{\text{SA}})$, with $\underline{U}_{\text{KA}}$ as defined in Section 4.2, and $\boldsymbol{\sigma}_{\text{SA}}$ as defined in Section 4.3.

5.2. Enhanced Drucker's error estimator

We will define the enhanced Drucker's error estimator by

$$e_T^{\text{ENH}} = \sup_{t \in [0,T]} \left(\int_\Omega \eta(\underline{M}, t, s_{\text{ad}}^{\text{ENH}})\, \mathrm{d}\Omega \right), \tag{19}$$

where $s_{\text{ad}}^{\text{ENH}} = (\underline{U}_{\text{KA}}, \boldsymbol{\sigma}_{\text{SA}}^{\text{ENH}})$, with $\underline{U}_{\text{KA}}$ as defined in Section 4.2, and $\boldsymbol{\sigma}_{\text{SA}}^{\text{ENH}}$ as defined in Section 4.4.

6. Practical construction of $\boldsymbol{\sigma}_{\text{SA}}^{\text{ENH}}(\underline{M}, t)$

This problem is clearly too complex to be solved exactly. Therefore, we will introduce some simplifications.

Following Ref. [15], the element tractions on the edges Γ of each element E are defined by a linear combination of the restriction on Γ of the shape functions $\omega_{j|\Gamma}$:

$$\widehat{\underline{F}}_h(t_i)_\Gamma = \underline{A}_\alpha^i \omega_{\alpha|\Gamma} + \underline{A}_\beta^i \omega_{\beta|\Gamma} + \sum_{j \in \bar{I}} \underline{A}_j^i \omega_{j|\Gamma}, \tag{20}$$

where

- the high-degree part $\sum_{j \in \bar{I}} \underline{A}_j^i \omega_{j|\Gamma}$ is completely defined by the weak prolongation condition (14),
- $\underline{A}_\alpha^i$ and $\underline{A}_\beta^i$ are the parameters

and (α,β) are the vertex nodes and $\bar{I}$ designates the set of the nonvertex nodes.

Let $\underline{A}^i$ be the column formed with all $\underline{A}_\alpha^i$ and $\underline{A}_\beta^i$. As $\widehat{\underline{F}}_h(t_i)$ must equilibrate the data, $\underline{A}^i$ must belong to a certain space designated by A_{ad}^i.

For fixed $\widehat{\underline{F}}_h(t_i)$, $\boldsymbol{\sigma}_{\text{SA}}^{\text{ENH}}(\underline{M}, t_i)_{|E}$ is built element by element. For simplicity, we use the same technique as the one developed in elasticity, and, as proposed in Ref. [15], we solve on each element E of the mesh an elasticity problem, where $\widehat{\underline{F}}_h(t_i)$ are the prescribed tractions on ∂E and F_d is the body force. This problem is solved by using a kinematic approximation of degree $p+3$ on E (where p is the degree on E of the current finite element approximation). This leads to a stress which is not strictly SA, but the error introduced by such an approximation is very small.

On each element E of the mesh we obtain

$$\boldsymbol{\sigma}_{\text{SA}}^{\text{ENH}}(\underline{M}, t_i)_{|E} = L_{|E}(\underline{A}^i) + \boldsymbol{\sigma}_d(\underline{M}, t_i)_{|E}, \tag{21}$$

where $\boldsymbol{\sigma}_d(\underline{M}, t_i)_{|E}$ depends on only the finite element solution and the data.

The optimal value for $(\underline{A}^i)_{i \in \{1,\ldots,n\}}$ is obtained by solving the minimization problem defined in Section 4.4 by Eq. (17).

To simplify the writing, we will consider plane stress problems. Let us designate by $\underline{\sigma} = \{\sigma_{xx}, \sigma_{yy}, \sqrt{2}\sigma_{xy}\}^{\mathrm{T}}$ and $\underline{\varepsilon} = \{\underline{\varepsilon}_{xx}, \underline{\varepsilon}_{yy}, \sqrt{2}\underline{\varepsilon}_{xy}\}^{\mathrm{T}}$, respectively, the vectors of stress and strain components;

- in order to make full use of the incremental method selected to solve the finite element problem, this minimization will be performed successively on each time increment. And we will minimize $e_{[0,t_i]}$ $\forall i \in \{1, \ldots, n\}$ instead of e_T,
- moreover, we assume that on $[t_{i-1}, t_i]$, $\underline{\sigma}_{\text{SA}}^{\text{ENH}}(\underline{M}, t_j)$ for $j < i$ is a data element for our minimization problem.

These assumptions lead to relatively simple calculations.

The problem then is to build

$$\underline{\sigma}_{\mathrm{SA}}^{\mathrm{ENH}}(t_i) \in \mathscr{S}_{\mathrm{ad},h}^{t_i} \text{ such that } \underline{\sigma}_{\mathrm{SA}}^{\mathrm{ENH}}(t_i) \text{ minimize } e^2[0,t_i]. \tag{22}$$

From Eqs. (7) and (9), it is easy to see that the error measure may be split into two parts:

$$e^2[0,t_i] = e^2[0,t_{i-1}] + \Delta a, \tag{23}$$

where

$$\Delta a = \sum_{E\in\mathbf{E}} \int_E \int_{t_{i-1}}^{t_i} (\underline{\sigma}_{\mathrm{SA}}^{\mathrm{ENH}} - \underline{\sigma}_{\mathrm{KA}})^{\mathrm{T}} (\dot{\underline{\varepsilon}}_{\mathrm{SA}} - \dot{\underline{\varepsilon}}_{\mathrm{KA}})\,\mathrm{d}t\,\mathrm{d}E. \tag{24}$$

Over the time interval $[t_{i-1},t_i]$, $e^2[0,t_{i-1}]$ is a data element of the minimization problem (22), which can be written:

$$\text{find } \underline{\sigma}_{\mathrm{SA}}^{\mathrm{ENH}}(t_i) \in \mathscr{S}_{\mathrm{ad},h}^{t_i} \text{ such that } \underline{\sigma}_{\mathrm{SA}}^{\mathrm{ENH}}(t_i) \text{ minimizes } \Delta a. \tag{25}$$

Remark. Δa is a scalar quantity which is not necessarily greater than zero because property (5) is satisfied only on $[0,t_{i+1}]$, but not on $[t_i,t_{i+1}]$.

For the elastoplasticity model, we can derive from the constitutive law (1) the following relation:

$$\dot{\underline{\sigma}}(t) = \mathbf{K}_{\mathrm{T}}(\underline{\sigma}(\tau);\ \tau\leqslant t)\ \dot{\underline{\varepsilon}}(t), \tag{26}$$

where $\mathbf{K}_{\mathrm{T}}(\underline{\sigma}(\tau);\ \tau\leqslant t)$ is the tangent modulus.

From the finite element solution, we obtain on $[t_{i-1},t_i]$:

$$\dot{\underline{\varepsilon}}_{\mathrm{KA}}(t) = \frac{\Delta\underline{\varepsilon}_h}{\Delta t}, \quad \underline{\sigma}_{\mathrm{KA}}(t) = \mathbf{A}(\underline{\varepsilon}_h(\dot{\underline{U}}\ (\tau));\ \tau\leqslant t), \tag{27}$$

where $\Delta t = t_i - t_{i-1}$ and $\Delta\underline{\varepsilon}_h = \underline{\varepsilon}_h(t_i) - \underline{\varepsilon}_h(t_{i-1})$.

Since we built $\underline{\sigma}_{\mathrm{SA}}^{\mathrm{ENH}}$ linearly on $[t_{i-1},t_i]$, it follows that

$$\begin{aligned} \underline{\sigma}_{\mathrm{SA}}^{\mathrm{ENH}}(t) &= \underline{\sigma}_{\mathrm{SA}}^{\mathrm{ENH}}(\underline{M},t_{i-1}) + \frac{t-t_{i-1}}{\Delta t}\ \Delta\underline{\sigma}_{\mathrm{SA}}^{\mathrm{ENH}}, \\ \dot{\underline{\varepsilon}}_{\mathrm{SA}}(t) &= \mathbf{K}_{\mathrm{T}}^{-1}\big(\underline{\sigma}_{\mathrm{SA}}^{\mathrm{ENH}}(\tau);\ \tau\leqslant t\big)\ \frac{\Delta\underline{\sigma}_{\mathrm{SA}}^{\mathrm{ENH}}}{\Delta t}. \end{aligned} \tag{28}$$

Let us now designate by $\Delta\mathscr{S}_{\mathrm{ad},h}^{t_i}$ the set of stresses that both satisfy

$$\int_E \big(\underline{\sigma}_{\mathrm{SA}}^{\mathrm{ENH}}(t_{i-1}) + \Delta\underline{\sigma}_{\mathrm{SA}}^{\mathrm{ENH}} - \underline{\sigma}_{\mathrm{KA}}(t_i)\big)^{\mathrm{T}}\,\underline{\varepsilon}(\underline{\omega}_j)\,\mathrm{d}\Omega = 0$$

and are in equilibrium with the load increment over $[t_{i-1},t_i]$.

By using Eqs. (27) and (28), Eq. (25) becomes

$$\text{find } \Delta\underline{\sigma}_{\mathrm{SA}}^{\mathrm{ENH}} \in \Delta\mathscr{S}_{\mathrm{ad},h}^{t_i} \text{ such that } \Delta\underline{\sigma}_{\mathrm{SA}}^{\mathrm{ENH}} \text{ minimizes } \sum_E \int_E \varphi_1(\Delta\underline{\sigma})\,\mathrm{d}E, \tag{29}$$

where

$$\begin{aligned} \varphi_1(\Delta\underline{\sigma}) = {}& \tfrac{1}{2}\Delta\underline{\sigma}^{\mathrm{T}}\,\mathbf{K}_p^{-1}\,\Delta\underline{\sigma} - \Delta\underline{\sigma}^{\mathrm{T}}[(\hat{\underline{\varepsilon}}_h^M + \tfrac{1}{2}\Delta\underline{\varepsilon}_h) \\ & - \mathbf{K}_m^{-1}\underline{\sigma}_{\mathrm{SA}}^{\mathrm{ENH}}(t_i)] + (\underline{\sigma}_h^M - \underline{\sigma}_{\mathrm{SA}}^{\mathrm{ENH}}(t_i))^{\mathrm{T}}\Delta\underline{\varepsilon}_h \end{aligned}$$

and

$$\mathbf{K}_p^{-1} = \frac{1}{\Delta t}\int_{t_{i-1}}^{t_i} \mathbf{K}_{\mathrm{T}}^{-1}(\underline{\sigma}(\tau);\ \tau\leqslant t)\,\mathrm{d}t,$$

$$\mathbf{K}_m^{-1} = \frac{2}{\Delta t}\int_{t_{i-1}}^{t_i} (t-t_{i-1})\,\mathbf{K}_{\mathrm{T}}^{-1}(\underline{\sigma}(\tau);\ \tau\leqslant t)\,\mathrm{d}t,$$

$$\hat{\underline{\varepsilon}}_h^M = \frac{1}{\Delta t}\int_{t_{i-1}}^{t_i} \mathbf{K}_{\mathrm{T}}^{-1}(\underline{\sigma}(\tau);\ \tau\leqslant t)\ \underline{\sigma}_{\mathrm{KA}}(t)\,\mathrm{d}t,$$

$$\underline{\sigma}_h^M = \frac{1}{\Delta t}\int_{t_{i-1}}^{t_i} \underline{\sigma}_{\mathrm{KA}}(t)\,\mathrm{d}t.$$

By using relation (21), problem (29) becomes

$$\begin{aligned} &\text{Find } (\underline{A}^i) \in A_{\mathrm{ad}}^i \text{ such that : } \underline{A}^i \text{ minimizes } J : \underline{A}^{i'} \\ &\qquad \mapsto J(\underline{A}^{i'}) \text{ on } A_{\mathrm{ad}}^i, \end{aligned} \tag{30}$$

where J is a nonlinear functional.

Problem (30) is a minimization problem with linear constraints which depends solely on $\underline{A}^i$ and which may be solved by using a conjugate gradient technique (with the initial guess for $\underline{A}^i$ given by the standard recovery method [4,5]. This problem is a priori global on the structure. However, in general, the initialization based on the standard method will be sufficient (for example, within the elastic zones), except for certain zones (near a singularity or within a transition zone between the plastic and elastic regions). It is not necessary to modify the standard Drucker's error on the entire structure. Therefore, the resolution of problem (30), by means of a conjugate gradient technique, will tend to be limited to only those zones causing difficulties. Moreover, our problem is not to find the exact stresses or the exact densities as solutions to problem (30), but rather to minimize the error on the constitutive relation overall. Just a few iterations of the gradient method will be sufficient to bring the error down to the desired level with an adequate degree of accuracy.

7. Examples

The following examples have been developed for plane stress problems. As the constitutive relation, we will be using a Prandtl–Reuss model for plasticity. There is only one internal variable p associated with the plastic strain. The spatial discretization uses six-node triangular elements.

7.1. Perforated plate: imposed loading

The perforated plate shown in Fig. 1 is submitted to a monotonous loading. We have performed a set of computations with a Young's modulus of $E = 200\,000$ MPa, a Poisson's ratio $v = 0.3$ and an isotropic hardening given by $R = Hp^{1/2}$ (the corresponding mesh is shown in Fig. 2). The plastic slope H/E varies from 0.1 to 0.001. For these slopes, the size of the plastic zone varies from 35% to 81% of the structure. When using the standard error estimator, the effectivity index (Fig. 3) varies from 3.5 to 4.5 as long as the slope is not less than 0.01; when the slope is very small (i.e., when approaching perfect plasticity), it is difficult to maintain an effectivity index of less than 5 and a value of 10 can be reached. If the enhanced error estimator were used, the effectivity index would vary from 2.1 to 2.8. It can be observed that this evolution is smoother than with the standard error estimator.

The evolutions of the errors as a function of the kinematic time can also be studied. We have represented these evolutions in Fig. 4 for a plastic slope of 0.1 and in Fig. 5 for a plastic slope of 0.005. When the plastic slope is high, the behavior of the errors is similar to linear elasticity; Fig. 6 reveals that the effectivity index is constant along the computation. When approaching a perfectly plastic behavior, the errors increase very fast and the effectivity index varies along the computation. The jump observed a the beginning of the plastification is due to the fact that the admissible stress begins to plastify before the FE stress. A significant improvement is obtained when using the enhanced construction, yet it is difficult to eliminate this phenomenon entirely.

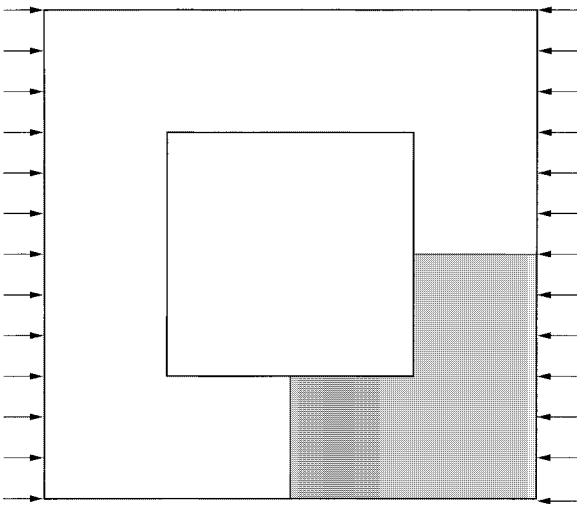

Fig. 1. Perforated plate.

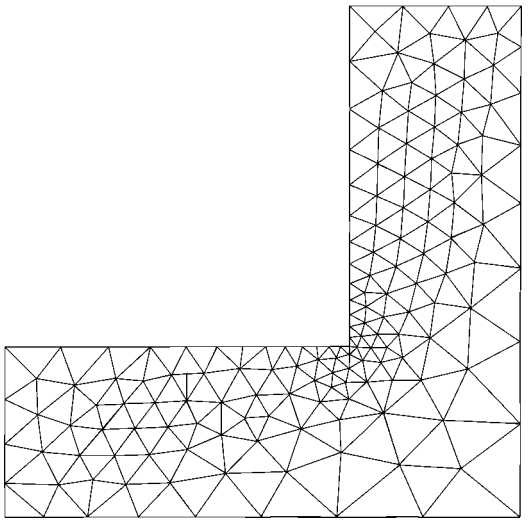

Fig. 2. Mesh used for the perforated plate: imposed loading.

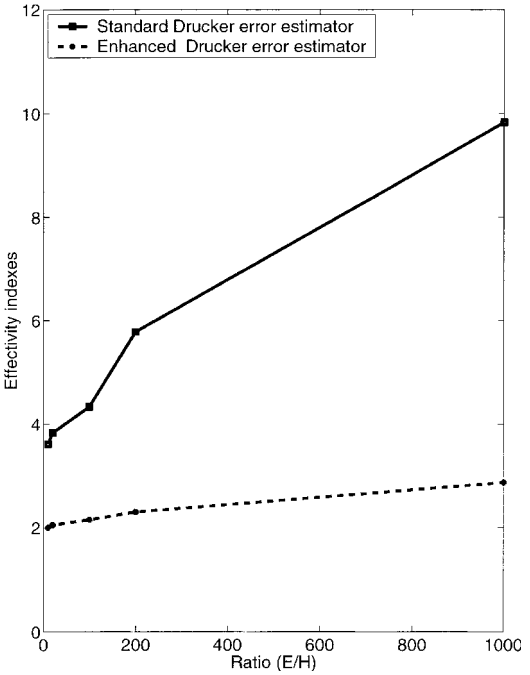

Fig. 3. Effectivity indexes versus E/H ratio.

7.2. Perforated plate: imposed displacement

The same plate used in Section 7.1 is studied herein. Loading is governed by prescribing displacement increments along the y-direction (the corresponding mesh is shown in Fig. 7). The computation has been performed with a Young's modulus of $E = 200\,000$ MPa, a Poisson's ratio $v = 0.3$ and an isotropic hardening given by $R = (E/1000)p^{1/2}$.

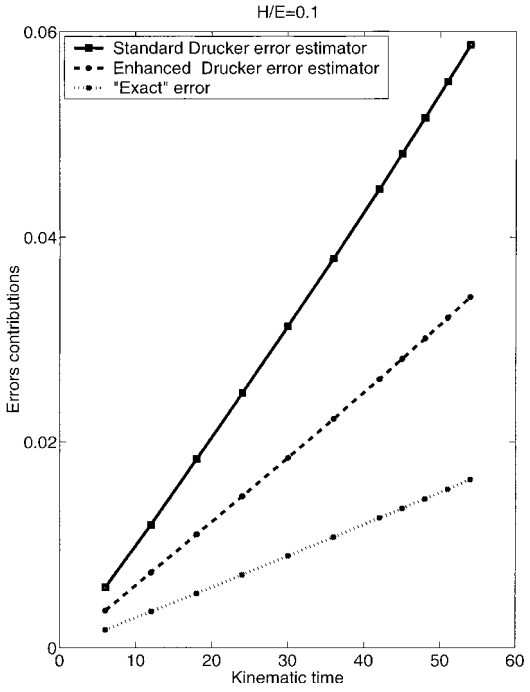

Fig. 4. Contributions to the error for a plastic slope of 0.1.

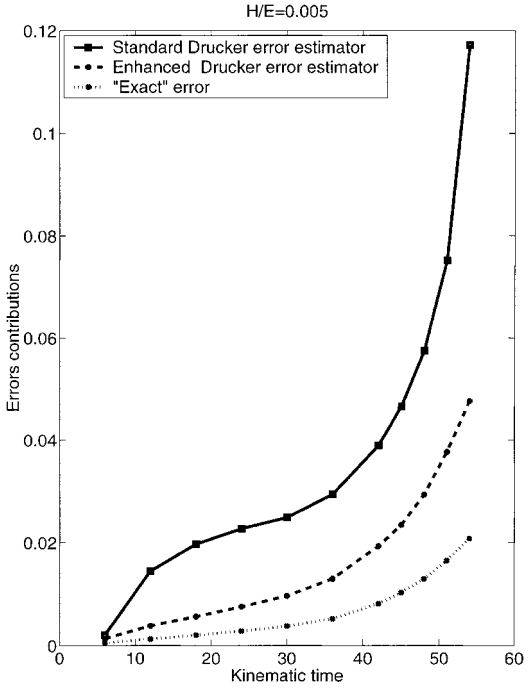

Fig. 5. Contributions to the error for a plastic slope of 0.005.

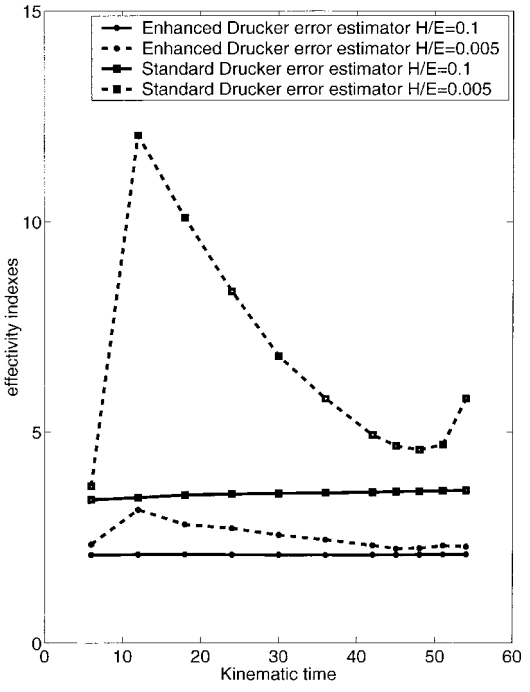

Fig. 6. Effectivity indexes versus kinematic time.

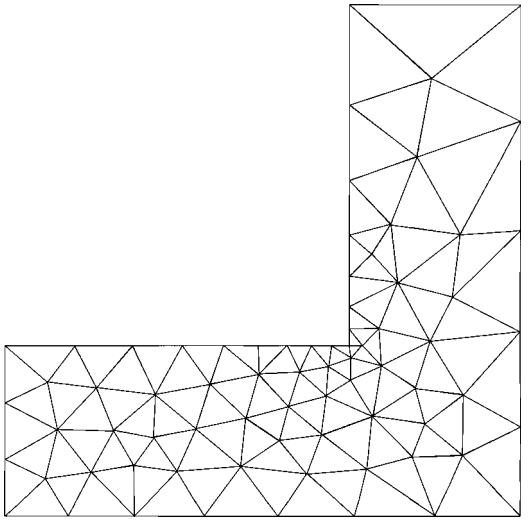

Fig. 7. Mesh used for the perforated plate: prescribed displacement.

Fig. 8 shows the evolution of the loading versus the imposed displacement. The limit load is reached around 3×10^{-2}. Fig. 9 shows the evolution of the contributions to the error, for both the standard error estimator and the enhanced error estimator. Fig. 10 displays the elements which contribute for 80% of the error improvement. Only 12 elements have been detected; they are located either near the singularity or near the limit of the plastic zone (Fig. 11). It will be sufficient to minimize

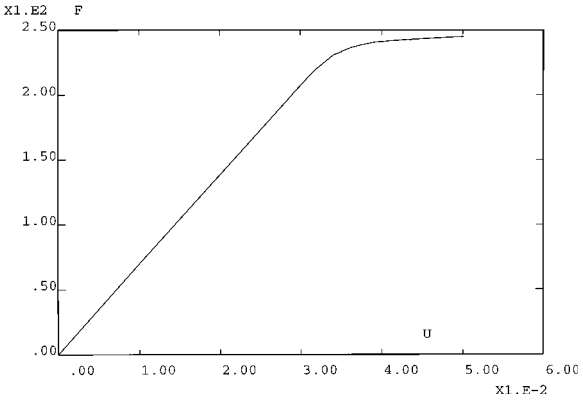

Fig. 8. Loading versus displacement.

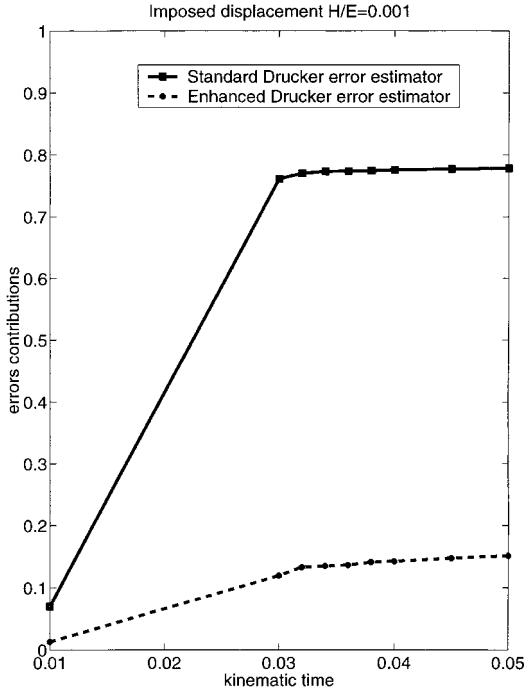

Fig. 9. Contributions to the error as a function of the kinematic time.

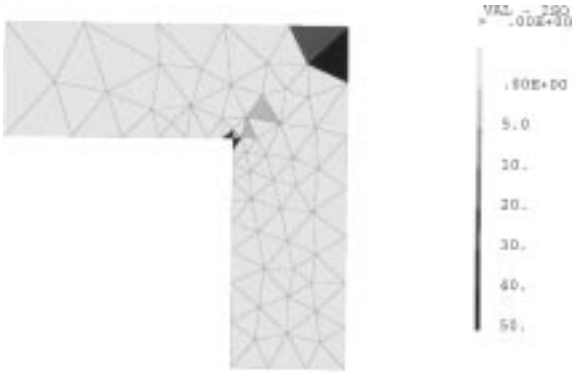

Fig. 10. Error improvement in %.

Fig. 11. Von Mises stress at the end of the loading.

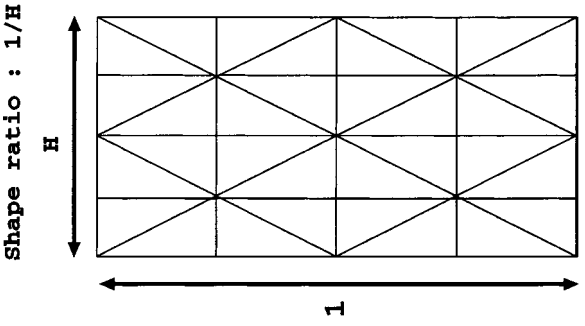

Fig. 12. Anisotropic mesh.

the error on only these elements and their neighboring elements, and then to use the standard construction for the other elements.

7.3. Calculation with an anisotropic mesh

We will use the example developed in Ref. [15]. The initial mesh is shown in Fig. 12, with the shape ratio $1/H$ as a parameter. The loading is monotonous. We have performed two sets of computations: the first in linear analysis, and the second with a Young's modulus $E = 200\,000$ MPa, a Poisson's ratio $v = 0.3$ and an isotropic hardening given by $R = 2000p^{1/2}$.

It appears that the new error estimator enables a real improvement in the effectivity index as the shape ratio increases (Fig. 13). If this result were compared with that obtained from the elastic computation, we would observe that the behavior of the effectivity index is very similar (Fig. 14). Fig. 15 represents the evolution of the

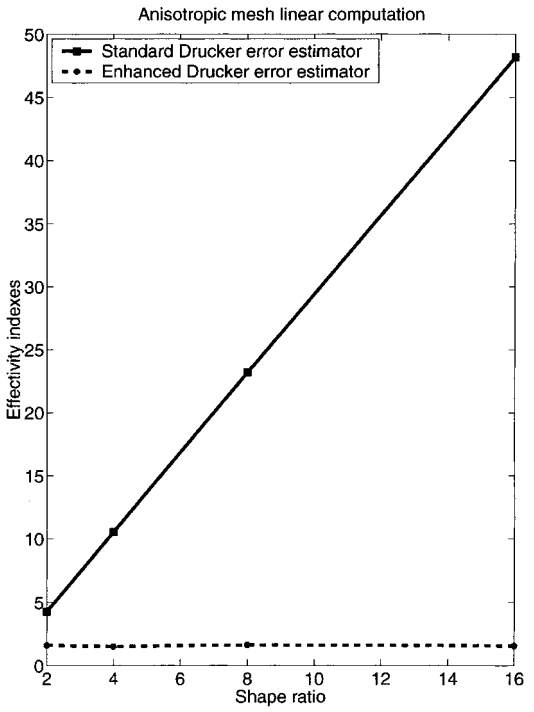

Fig. 13. Effectivity index in elastoplasticity versus shape ratio for the standard and enhanced error estimators.

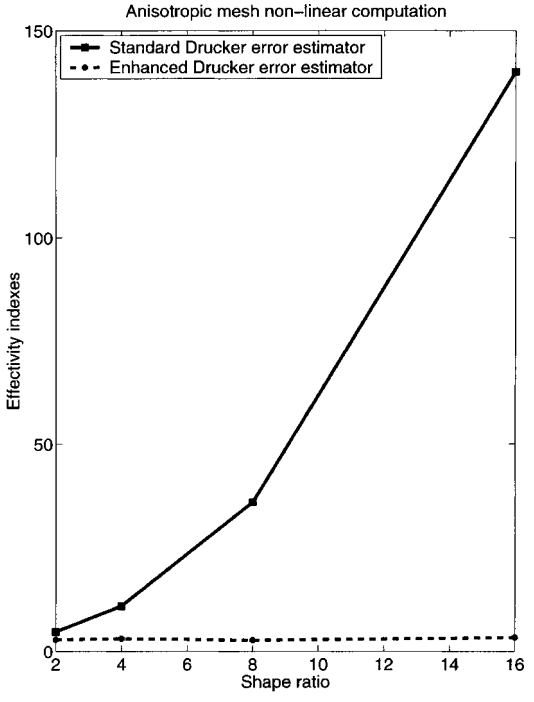

Fig. 14. Effectivity index in elasticity versus shape ratio for the standard and enhanced error estimators.

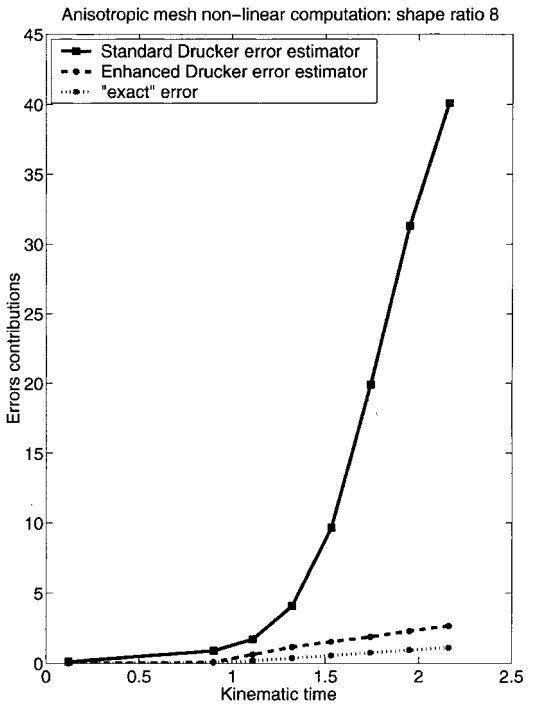

Fig. 15. Contribution to the error versus kinematic time.

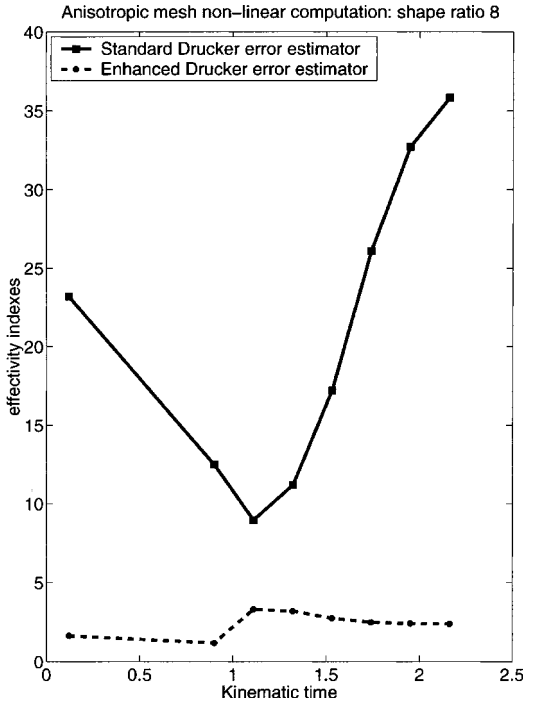

Fig. 16. Effectivity index versus kinematic time.

errors as a function of the kinematic time for a shape ratio of 8. The behavior of both the *exact* error and the enhanced error estimator seems to be similar. This observation is confirmed in Fig. 16, where the effectivity index has been drawn as a function of the kinematic time.

8. Conclusion

An enhanced error estimator on the constitutive relation for elastoplasticity problems has been presented here. By introducing a minimization of the error on the constitutive relation on a set of admissible stresses, we have built an enhanced admissible stress field $\boldsymbol{\sigma}_{SA}^{ENH}$ which is nearer to the exact stress field than the standard admissible stress field $\boldsymbol{\sigma}_{SA}$. $\boldsymbol{\sigma}_{SA}^{ENH}$ is used to define the enhanced error estimator. Thus, in the case where a slight difference between the admissible stress field and the exact stress field leads to an important variation of the calculated error (quasi-perfect plasticity) or when the standard admissible field is far from the exact stress field (anisotropic mesh), this enhanced error estimator leads to great improvement of the effectivity index. Such an error estimator can easily be developed for viscoplasticity problems. The extension to a dissipation error estimator, as developed in Refs. [12,13], could also be performed following the same technique.

References

[1] Bass JM, Oden JT. Adaptative finite element methods for a class of evolution problems in viscoplasticity. Int J Engng Sci 1987;25(6):623–53.

[2] Boroomand B, Zienkiewicz OC. Recovery procedures in error estimation and adaptivity: adaptivity in nonlinear problems of elasto-plasticity behaviour. In: Ladevèze P, Oden JT, editors. Advances in adaptive computational methods in mechanics. Studies in applied mechanics vol. 47, Amsterdam: Elsevier; 1998. p. 383–410.

[3] Drucker DC. On the postulate of stability of material in the mechanics of continua. Journal de Mécanique 1964; 3(2):235–49.

[4] Gallimard L, Ladevèze P, Pelle JP. Error estimation and adaptivity in elastoplasticity. Int J Num Meth Engng 1996;39:189–217.

[5] Gallimard L, Ladevèze P, Pelle JP. Error estimation and time-space parameters optimization for fem non-linear computation. Comput Struct 1997;64:145–56.

[6] Larsson R, Jin H, Bernspang L, Wiberg NE. Mesh generation and mesh refinement procedures for computional plasticity. Proc Int Conf Comp Plas, Barcelonne, 1990. p. 347–58.

[7] Ladevèze P. Nouvelles procédures d'estimations d'erreur relative à la méthode des éléments finis. Proc Journées Eléments finis, Rennes, 1977.

[8] Ladevèze P. Sur une famille d'algorithmes en mécanique des structures. C Rendus Acad Sci Paris, Sér II 1985; 300:41–4.

[9] Ladevèze P. Nonlinear computational structural mechanics. New approaches and non-incremental methods of calculations. Mechanical Engineering Series, Berlin: Springer; 1999.

[10] Ladevèze P, Coffignal G, Pelle JP. 1986. Accuracy of elastoplastic and dynamic analysis. In: Babuška I, Gago J, Oliveira ER de A, Zienkiewicz OC, editors. Accuracy estimates and adaptive refinements in finite element computations, New York: Wiley; 1986. p. 181–203.

[11] Ladevèze P, Leguillon D. Error estimate procedure in the finite element method and application. SIAM J Num Anal 1983;20(3):485–509.

[12] Ladevèze P, Moës N. A new a posteriori error estimation for nonlinear time-dependent finite element analysis. Comp Meth Appl Mech Engng 1997;157:45–68.

[13] Ladevèze P, Moës N. A posteriori constitutive relation error estimators for nonlinear finite element analysis and adaptive control. In: Ladevèze P, Oden JT, editors. Advances in adaptive computational methods in mechanics. Studies in applied mechanics, vol. 47. Amsterdam: Elsevier; 1998. p. 231–56.

[14] Ladevèze P, Pelle JP, Rougeot P. Error estimation and mesh optimization for classical finite elements. Engng Computat 1991;8:69–80.

[15] Ladevèze P, Rougeot P. New advances on a posteriori error on constitutive relation in f.e. analysis. Comp Meth Appl Mech Engng 1997;150:239–49.

[16] Owen DRJ, Hinton E. Finite elements in plasticity. Swansea (UK): Pineridge; 1986.

[17] Peric D, Yu J, Owen DRJ. On error estimates and adaptivity in elasto-plastic solids: applications to the numerical simulation of strain localisation in classical and Cosserat continua. Int J Num Meth Engng 1994; 37:1351–79.

[18] Rannacher R, Stuttmeier FT. A posteriori error control and meah adaptation for f.e. models in elasticity and elastoplasticity. In: Ladevèze P, Oden JT, editors. Advances in adaptive computational methods in mechanics. Studies in applied mechanics, vol. 47. Amsterdam: Elsevier; 1998. p. 275–92.

[19] Stein E, Barthold FJ, Ohnimus S, Schmidt M. Adaptive finite element in elastoplasticity with mechanical error indicators and neumann-type estimators. In: Ladevèze P, Oden JT, editors. Advances in adaptive computational methods in mechanics. Studies in applied mechanics, vol. 47. Amsterdam: Elsevier; 1998. p. 81–100.

[20] Tie B, Aubry D. Error estimates, h adaptive strategy and hierarchical concept for nonlinear finite element method. In: Hirsch et al. editors. Numerical Methods in Engineering '92. Amsterdam: Elsevier; 1992. p. 17–24.

[21] Zienkiewicz OC, Liu YC, Huang GC. Error estimation and adaptivity in flow formulation for forming problems. Int J Num Meth Engng 1988;25:23–42.